DOE/MC/31224 -- 5514
Distribution Category UC-132

Naturally Fractured Tight Gas Reservoir Detection Optimization

Quarterly Report
Juyly 1 - September 30, 1996

Work Performed Under Contract No.: DE-AC21-94MC31224

For
U.S. Department of Energy
Office of Fossil Energy
Morgantown Energy Technology Center
P.O. Box 880
Morgantown, West Virginia 26507-0880

By
Blackhawk Geometrics
301 Commercial Road
Suite B
Golden, Colorado 80401

Disclaimer

1.0 3-D 3-C PROCESSING

The 3-D 3-C dataset recorded in October, 1995, is being processed at Western Geophysical in their Denver office. Western is currently processing both the P-P and P-S datasets. In addition to Western's familiarity with the processing flow established for the 37 square mile 3-D, their research department is currently developing a fractogram technique to detect the orientation and density of fracturing for 3-D data. Western has agreed to test the fractogram on the DOE dataset.

1.1 P-P Processing

The processing of the P-P data began in April, 1996, and has progressed to the point where the fractogram analysis can begin. The basic processing flow for the P-P portion of the 3-D 3-C dataset was modeled closely after the processing sequence performed on the 37 square mile 3-D data. A new methodology of processing has been proposed for post-NMO data to take full advantage of the insights gained in the 37 square mile 3-D, and the relatively complete azimuth and offset distribution available in the 3-D 3-C survey. The processing flow is outlined below. Processes performed during this reporting period are shown in boldface type.

Structural Stack	Fractogram Analysis
Geometry Description for V, H1 and H2 Components	
Amplitude Recovery Using $T^{1.5}$ Exponential Gain	
RAAC (Residual Amplitude Analysis/Compensation)	
Surface Consistent Deconvolution	
Refraction Statics	
Velocity Analysis	
MISER Reflection Statics	
Iterations of Steps VI and VII to Convergence	
Dip Moveout Application	
DMO Velocity Analysis	
Output data to Fractogram Analysis	**All azimuths with final statics and current velocities**
Stack	**Separate data in 4 azimuth volumes as follows:** **0 deg. (+/- 22.5 deg)** **45 deg (+/- 22.5 deg.)** **90 deg. (+/- 22.5 deg.)** **135 deg. (+/- 22.5 deg.)**
Migrate	Run DMO monitors at selected locations for velocity analysis for each volume
	Pick DMO velocities for each volume (limit far offsets as below)
	Divide volumes from (2) into near (0 to 3000 ft.) and far (3000 to ~7000 ft.) offset volumes for a total of 8 volumes. (3000 ft ~ 15 deg. at 1.2 sec)
	Calculate EQ DMO weights for all 8 volumes individually
	Progressive EQ DMO and Stack for all 8 volumes Near offsets may be done at 110 ft. by 220 ft. cell size to improve fold
	Time Migration of all 8 volumes (Extended Stolt - single velocity function)
	Provide client with 8 volumes for interpretation
	Develop amplitude scalar field from near offset volumes Calculate amplitude envelope volumes Spatial and temporal averaging Interpolation back to 110 ft by 110 ft cell Sum 4 smoothed volumes, output average volume Divide average envelope volume by individual envelope volumes Create ratio volume for each of 4 volumes
	Normalize far offset volumes - multiply by appropriate ratio volumes
	Run fractogram analysis with normalized far offset volumes
	Provide client Φ and B/A volumes for interpretation

1.2 P-S Processing

Processing of the P-S wave data began in June, 1996. Western Geophysical is still finishing the code for some of the processes, but the project is progressing satisfactorily and is on track to be finished by December 15, 1996. As the DOE project is the first converted wave processing attempted by Western, many modules of the processing flow are still under development. The steps that were accomplished during this quarter are shown in boldface type.

S1 and S2 Structural Stacks
Geometry Description for V, H1 and H2 Components
Rectification of Trace Polarity with Azimuth
Amplitude Recovery Using $T^{1.5}$ Exponential Gain Function
RAAC (Residual Amplitude Analysis/Compensation)
Zone Anomaly Processing on H1 and H2 Separately
FXCNS (Coherent Noise Suppression Performed in f-x Space)
Surface Consistent Deconvolution **i) Apply source term derived from P-P processing.** **ii) Calculate receiver and source terms using azimuth limited H1 and H2 data.** **iii) Apply receiver and offset terms to H1 and H2.**
Apply Source Refraction Statics Derived from P-P Processing
Rotation Analysis to Determine H1' and H2'
Apply Rotation to Both Volumes
Velocity Analysis
Residual Statics
Common Conversion Point (CCP) Binning
Iteration of velocities, Statics and CCP Binning until Convergence is Reached
CCP Trim Statics (if needed)
CCP Stack
Wave Separation/Layer Stripping
Random Noise Attenuation
Time Migration

2.0 CORRELATION MATRIX

The two seismic datasets (North-South and East-West) from the 37 square mile 3-D have been interpreted for the following horizons:

- Top of the Waltman Shale
- Top of the Lower Fort Union (LFU)
- Base of the LFU

From these interpreted horizons, certain seismic attributes can be determined for the LFU for both the NS and EW datasets. A comparison of the two datasets will show areas of anomalous seismic behavior. These areas will then be correlated with production data from the wells in the survey area to determine which attribute anomalies correspond to gas pay.

The anomalies under study fall into two classes, reflection anomalies and transmission anomalies. These anomaly types are illustrated in Figure 2-1.

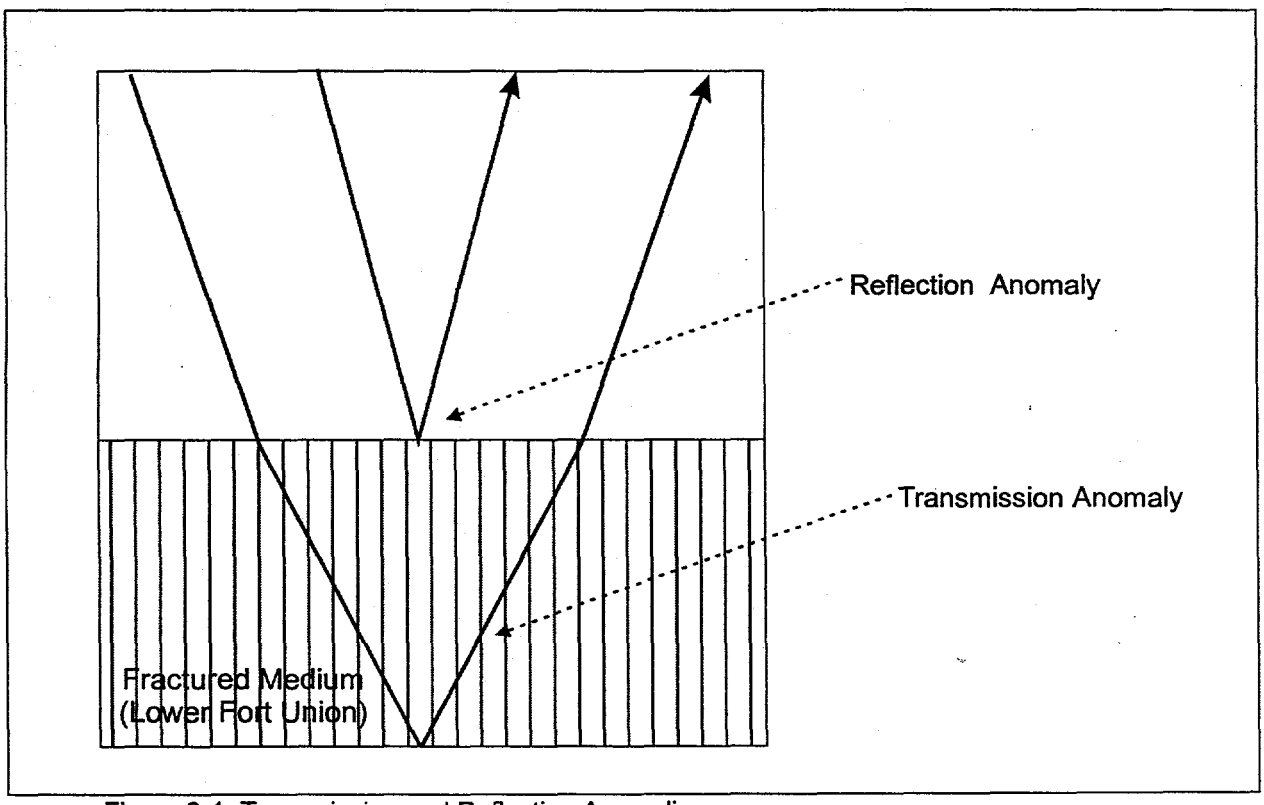

Figure 2-1 Transmission and Reflection Anomalies

The reflection anomalies studied in the correlation matrix are:

- Difference in Reflection Strength (NS-EW)
- Sum of AVO Gradients (NS+EW)
- Difference of AVO Gradients (NS-EW)

The transmission anomalies under study in the project are:

- Interval Velocity Ratio (NS/EW) Top 1/2 of the LFU
- Seismic Frequency Difference (NS-EW) Top 1/2 of the LFU

Figure 2-2 shows the extent of the 37 square mile survey and the locations of the axis and crest of the anticline in the Wind River Basin study area. A discussion of the attributes is given below, and as the area of gas production from fractures is mainly located on the crest of the anticline, the discussion of attributes will be concentrated there.

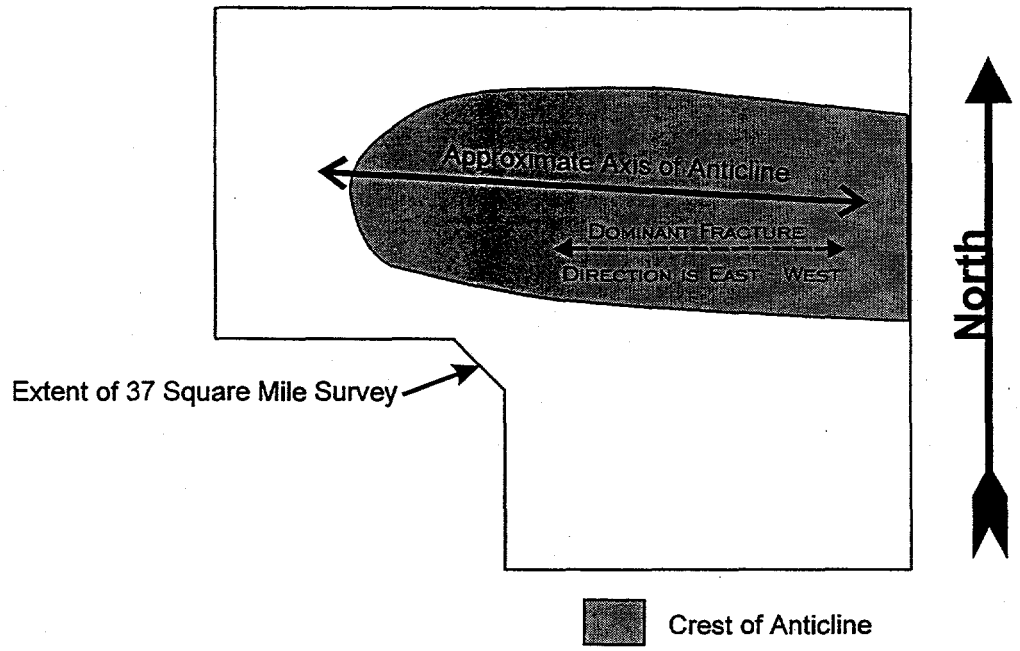

Figure 2-2 Location Map of the Anticline in the Wind River Basin 3-D Study Area

2.1 Ratio of Interval Velocities

Theory predicts that compressional seismic waves which travel parallel to the dominant fracture direction (EW) will not sense the EW fractures and travel at matrix velocities, while compressional seismic waves which travel perpendicular to the dominant fracture direction will sense the maximum influence of the EW fractures, and travel at a slower velocity.

In areas of intense EW fracturing, the interval velocity of the LFU in the NS volume is expected to be lower than the interval velocity of the LFU in the EW volume. Since we divided the NS velocity field by the EW velocity field, these areas of EW fracturing are represented by interval velocity ratios less than one. Figure 2-3 shows the "Ratio of interval velocity map" for the Lower Fort Union. Warm colors (yellows and reds) correspond to ratios of less than one, and several of these areas appear along the crest of the structure.

In general, all seismic attribute maps presented in this report were designed to show warm colors where EW fractures are indicated or interpreted to exist.

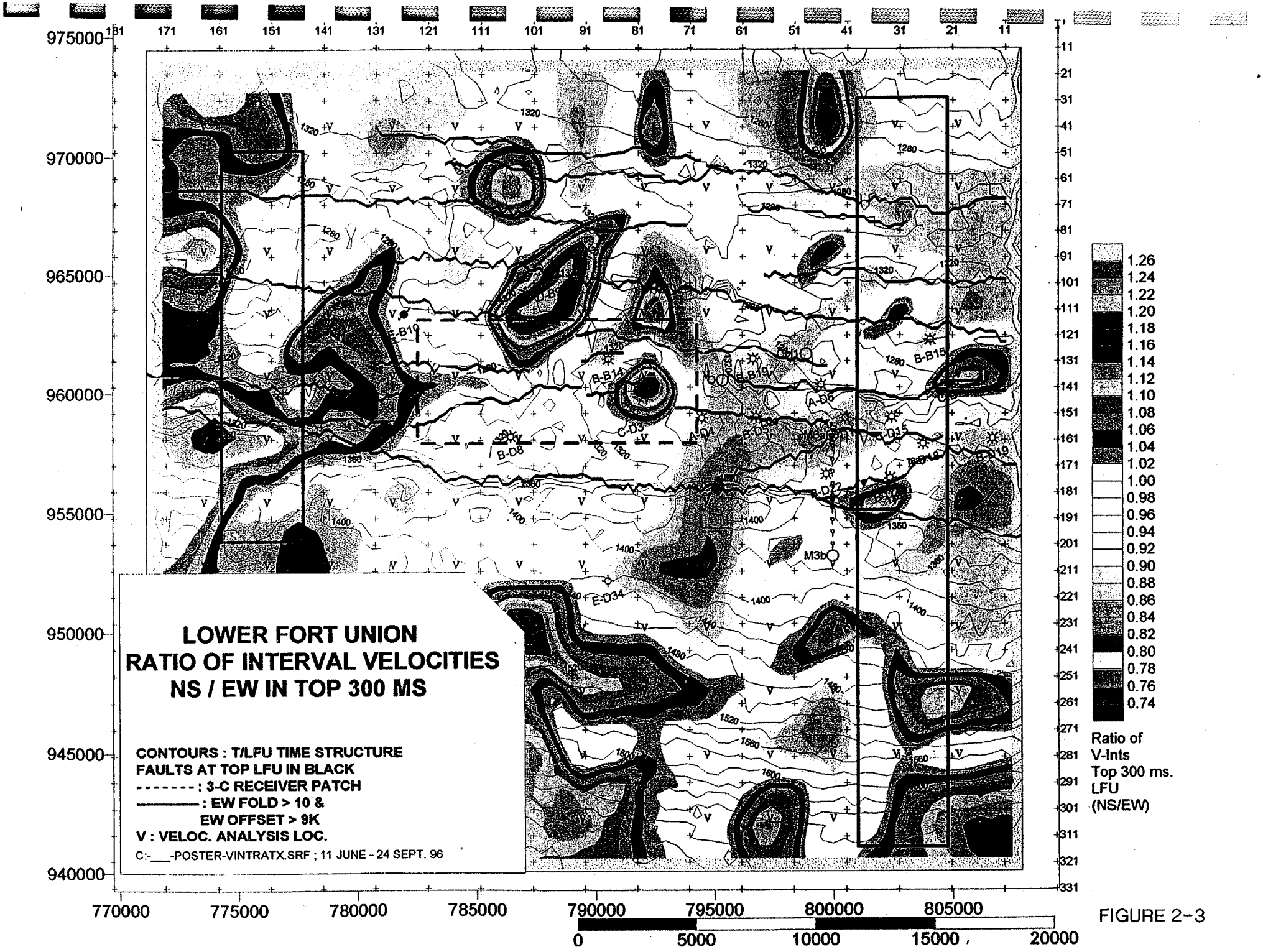
LOWER FORT UNION
RATIO OF INTERVAL VELOCITIES
NS / EW IN TOP 300 MS
CONTOURS : T/LFU TIME STRUCTURE
FAULTS AT TOP LFU IN BLACK
- - - - - - - : 3-C RECEIVER PATCH
———— : EW FOLD > 10 &
EW OFFSET > 9K
V : VELOC. ANALYSIS LOC.
C:-___-POSTER-VINTRATX.SRF ; 11 JUNE - 24 SEPT. 96
1.26
1.24
1.22
1.20
1.18
1.16
1.14
1.12
1.10
1.08
1.06
1.04
1.02
1.00
0.98
0.96
0.94
0.92
0.90
0.88
0.86
0.84
0.82
0.80
0.78
0.76
0.74
Ratio of
V-Ints
Top 300 ms.
LFU
(NS/EW)
975000
970000
965000
960000
955000
950000
945000
940000
770000
775000
780000
785000
790000
795000
800000
805000
0
5000
10000
15000
20000

FIGURE 2-3

2.2 Difference in Interval Average Frequency

As with interval velocity, the frequency of a reflected seismic wave will be lowered as it crosses fractures. From this, the N-S data volume should exhibit lower frequencies than the E-W volume in areas of intense E-W fracturing.

The average frequency of the seismic wavetrain was calculated for each volume in a 300 msec interval at the top of the LFU. The average interval frequency of the EW volume was subtracted from the average interval frequency of the NS volume. In areas of EW fracturing, the NS minus EW data should show a negative number. Figure 2-4 shows the negative numbers in warm colors. An examination of Figure 2-4 shows a high concentration of negative values along the crest of the anticline on the Eastern half of the map.

2.3 Sum of AVO Gradients

The Amplitude Variation with Offset (AVO) parameter is generally given as a relationship where the amplitude vs. offset is described by :

$$\text{Amplitude} = A + B(x)$$

Where A represents the zero intercept and B is the gradient (or slope). For the Top of the Lower Fort Union, where a faster sand underlies a slower shale the expected AVO relationships for the E-W and N-S datasets are shown on Figure 2-5.

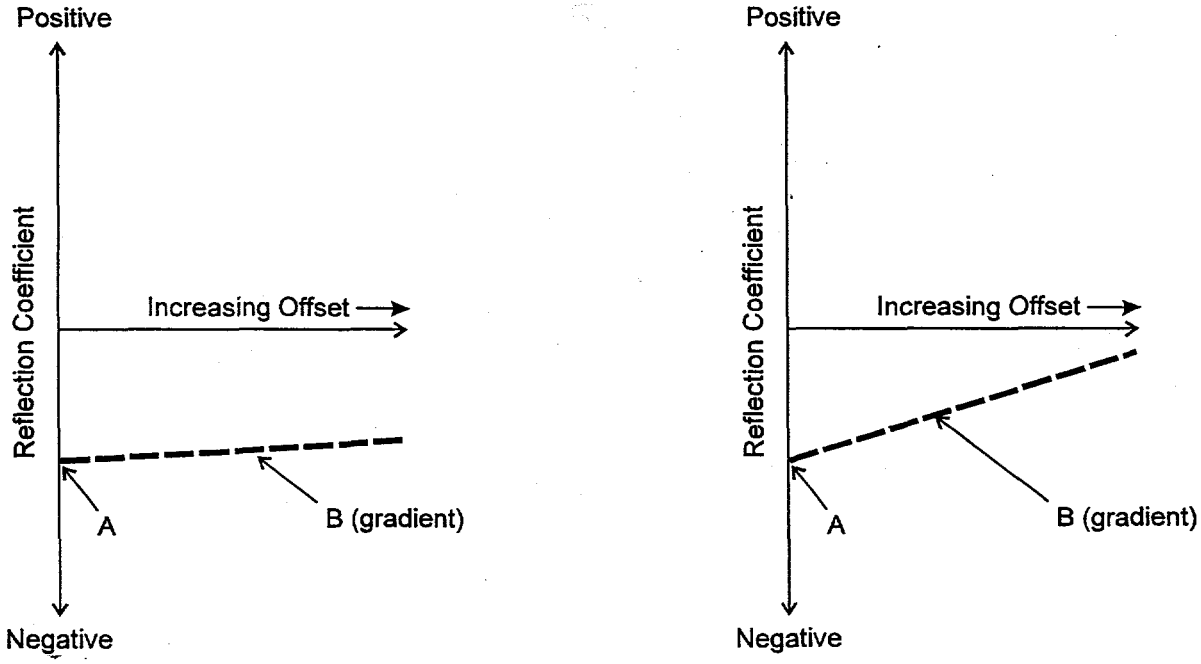

a) AVO for E-W dataset

b) AVO for N-S dataset

Figure 2-5 AVO response for raypaths traveling a) parallel to, and b) perpendicular to the dominant fracture direction (Personal Communication, Leon Thomsen; see also Leading Edge, August 1996, Bluebell-Altamont, UT Paper)

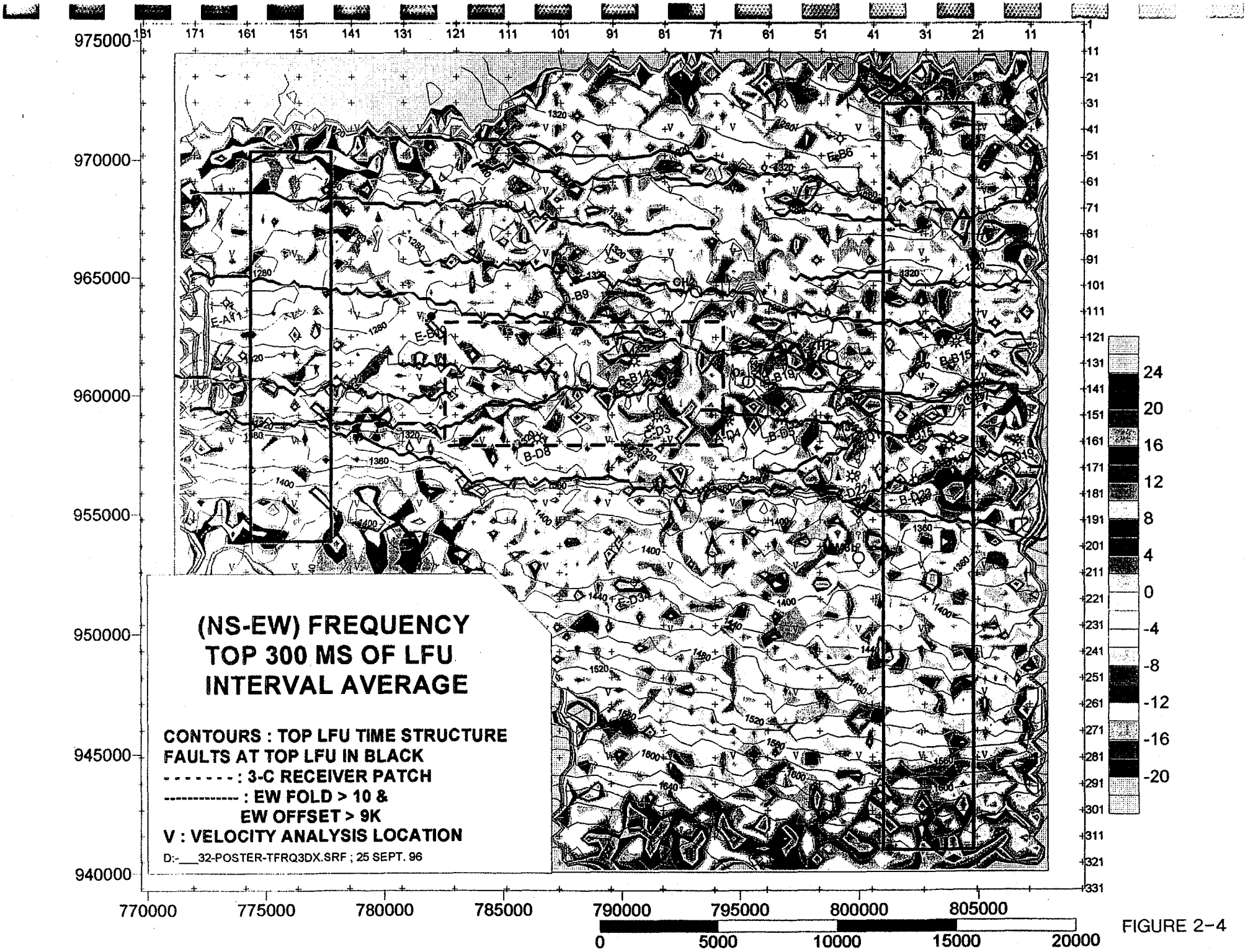
(NS-EW) FREQUENCY
TOP 300 MS OF LFU
INTERVAL AVERAGE
CONTOURS : TOP LFU TIME STRUCTURE
FAULTS AT TOP LFU IN BLACK
- - - - - - - : 3-C RECEIVER PATCH
---------- : EW FOLD > 10 &
EW OFFSET > 9K
V : VELOCITY ANALYSIS LOCATION
D:-___32-POSTER-TFRQ3DX.SRF ; 25 SEPT. 96
975000
970000
965000
960000
955000
950000
945000
940000
770000
775000
780000
785000
790000
795000
800000
805000
0
5000
10000
15000
20000
24
20
16
12
8
4
0
-4
-8
-12
-16
-20

FIGURE 2-4

A positive AVO gradient is interpreted to indicate a decrease in Poisson Ratio, which is consistent with the presence of a gas sand under a shale. If fractures are present, the AVO gradient parallel to the fractures is sensitive to matrix porosity and pore contents, while the AVO gradient perpendicular to the fractures is sensitive to matrix porosity and content, and fracture content (if gas). If the sum of the two gradients is positive, it is an indication that either both gradients are positive, or one of the gradients is positive enough to dominate the sum.

Figure 2-6 shows the Sum of AVO gradient map. The positive values (shown again as warm colors) are consistent with a decreased Poisson's Ratio at the top of the LFU, which is consistent with the presence of gas in the top of the LFU. Many areas corresponding to positive AVO gradient sum are located along the crest of the structure.

2.5 Difference of AVO Gradients

If the difference (NS-EW) of the AVO gradients is positive, it means that the NS AVO gradient is greater than the EW AVO gradient. From the discussion above, this relationship is consistent with EW cracks. Figure 2-7 shows difference in AVO gradient as warm colors when positive. An examination of Figure 2-7 shows a concentration of positive anomalies along the crest of the structure.

2.6 Difference in Reflection Strength

As the reflection at the Top of the Lower Fort Union is a trough, it is evident from Figure 2-5 that the stack response for the EW volume will be a deeper (or more negative) trough than for the NS dataset in the presence of fractures. To simplify analysis, we use reflection strength (the absolute value of reflection amplitude) for our comparison. In the presence of EW fractures, when the EW trough (large value) is subtracted from the NS trough (smaller value), a negative value is the expected result.

Figure 2-8 shows the negative values for difference in reflection strength as warm colors, and again a strong concentration of positive values is seen along the crest of the anticline.

2.7 Correlation

The correlation of the seismic anomalies with the production information was accomplished by first ranking the Estimated Ultimate Recovery (EUR) of all wells in the survey area into five categories. Table 2-1 shows the categories established by the industry partner.

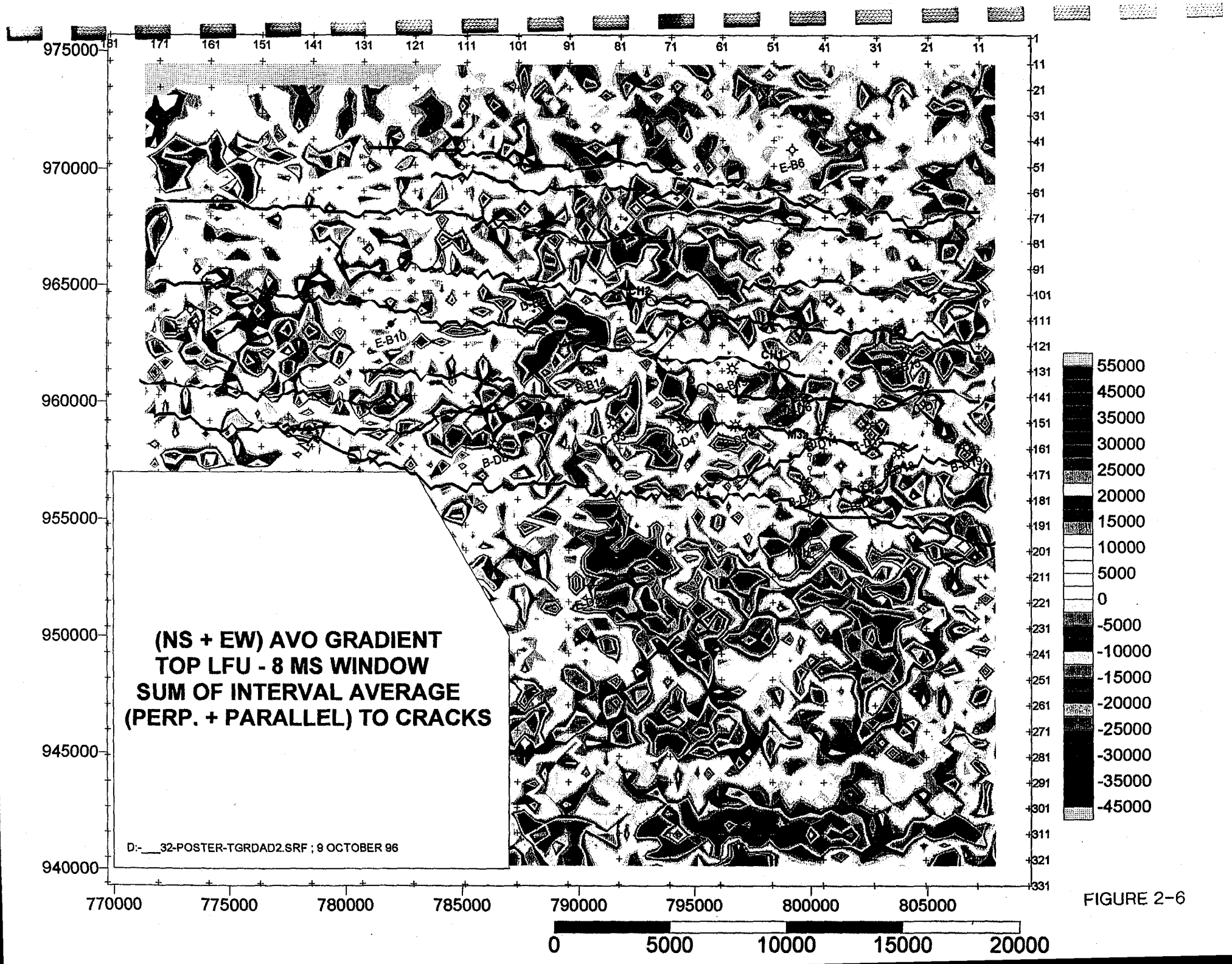
(NS + EW) AVO GRADIENT
TOP LFU - 8 MS WINDOW
SUM OF INTERVAL AVERAGE
(PERP. + PARALLEL) TO CRACKS
D:-___32-POSTER-TGRDAD2.SRF ; 9 OCTOBER 96
55000
45000
35000
30000
25000
20000
15000
10000
5000
0
-5000
-10000
-15000
-20000
-25000
-30000
-35000
-45000
975000
970000
965000
960000
955000
950000
945000
940000
770000
775000
780000
785000
790000
795000
800000
805000
0
5000
10000
15000
20000

FIGURE 2-6

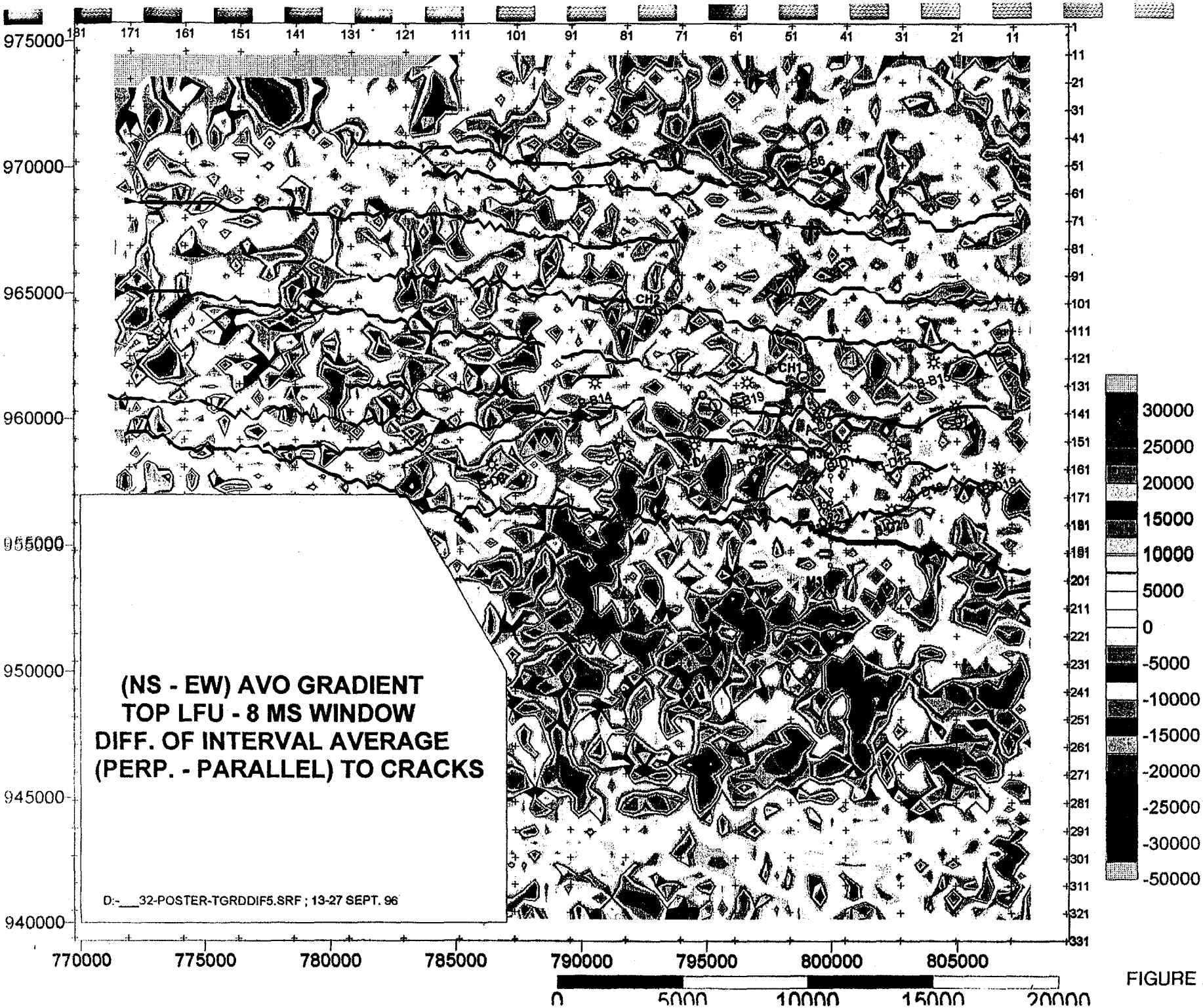
(NS - EW) AVO GRADIENT
TOP LFU - 8 MS WINDOW
DIFF. OF INTERVAL AVERAGE
(PERP. - PARALLEL) TO CRACKS
D:-___32-POSTER-TGRDDIF5.SRF ; 13-27 SEPT. 96
975000
970000
965000
960000
955000
950000
945000
940000
770000
775000
780000
785000
790000
795000
800000
805000
30000
25000
20000
15000
10000
5000
0
-5000
-10000
-15000
-20000
-25000
-30000
-50000
0
5000
10000
15000
20000

FIGURE 2-7

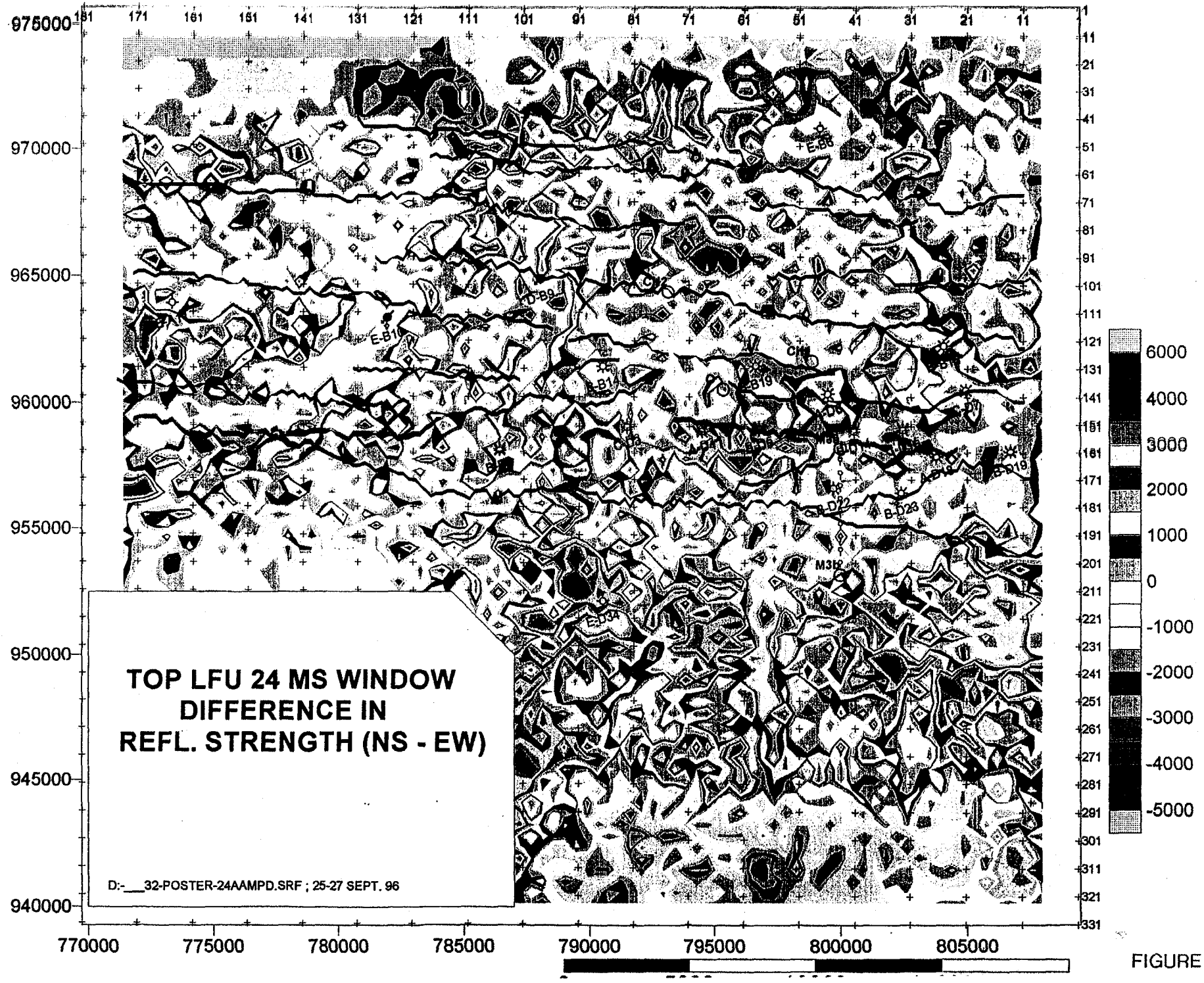
TOP LFU 24 MS WINDOW
DIFFERENCE IN
REFL. STRENGTH (NS - EW)
D:-___32-POSTER-24AAMPD.SRF ; 25-27 SEPT. 96
975000
970000
965000
960000
955000
950000
945000
940000
770000
775000
780000
785000
790000
795000
800000
805000
6000
4000
3000
2000
1000
0
-1000
-2000
-3000
-4000
-5000

FIGURE 2-8

Table 2-1

Category	Range of Estimated Ultimate Recovery
A	> 15 Billion Cubic Feet (BCF)
B	8 BCF to 15 BCF
C	1 BCF to 8 BCF
D	0 BCF to 1 BCF
E	Non-Commercial / Non-Productive

Figure 2-9 is a chart of interval velocity at each well. The well names are listed along the top, and each well's production ranking is listed below it along the bottom. The pink and green lines represent the seismic velocity at each well location for the EW and NS volumes, respectively. The seismic velocity at each well can be read from the axis on the left side of the chart. The gray line represents the interval velocity ratio, and this line corresponds to the axis on the right side of the page. The area in between the red and blue lines is labeled as isotropic, as the values between these lines are close to 1.0, meaning little difference exists between NS and EW. The ratio values below 0.95 are considered "Prospective" in that the EW interval velocities are significantly greater than the NS interval velocities. The points which lie above the isotropic area are considered "Non-prospective". This chart shows that for 10 of the 12 excellent wells (Category A or B) show a prospective interval velocity.

Table 2-2 lists the seismic attributes discussed above against the Category A and B wells. This table shows good agreement between the seismic anomalies and gas production.

Further analysis of the relationships between the seismic attributes and EUR is underway and will be detailed in future reports.

"PROSPECTIVE" ANISOTROPY = "Positive" Seismic Fingerprint

	WELL NAME	INT. VEL. RATIO	INT. FREQ. DIFF.	AVO SUM	AVO DIFF.	DIFF. REFL. STRENGTH	# OF "PROSP." ATT. PRESENT	# OF "NON-PROSP." ATT. PRESENT
	A-D18	✓	AMB	✓	✓	--	3/5	1/5
	A-D6	✓	✓	--	--	✓	3/5	2/5
	A-D4	✓	✓	✓	✓	✓	5/5	0/5
	B-B15	✓	--	--	✓	✓	3/5	2/5
	B-B14	✓	AMB	✓	✓	--	3/5	1/5
	B-D22	✓	✓	✓	✓	AMB	4/5	0/5
	B-D5	✓	✓	✓	✓	✓	5/5	0/5
	B-D23	AMB	--	✓	--	--	1/5	3/5
	B-B19	✓	✓	✓	✓	✓	5/5	0/5
	B-D14	✓	--	✓	--	--	2/5	3/5
	B-D8	AMB	--	--	--	--	[1]/5	4/5
	B-D19	✓	--	--	✓	AMB	2/5	2/5

✓ = "PROSPECTIVE" ATT. PRESENT

-- = "PROSPECTIVE" ATT. NOT PRESENT

AMB = AMBIGUOUS

5/5 PROSPECTIVE ATTRIBUTES: 3/12 WELLS 25%
4/5 PROSPECTIVE ATTRIBUTES: 1/12 WELLS 8%
3/5 PROSPECTIVE ATTRIBUTES: 4/12 WELLS 33%
2/5 PROSPECTIVE ATTRIBUTES: 2/12 WELLS 17%
3+/5 PROSPECTIVE ATTRIBUTES: 8/12 WELLS 66%

TABLE 2-2

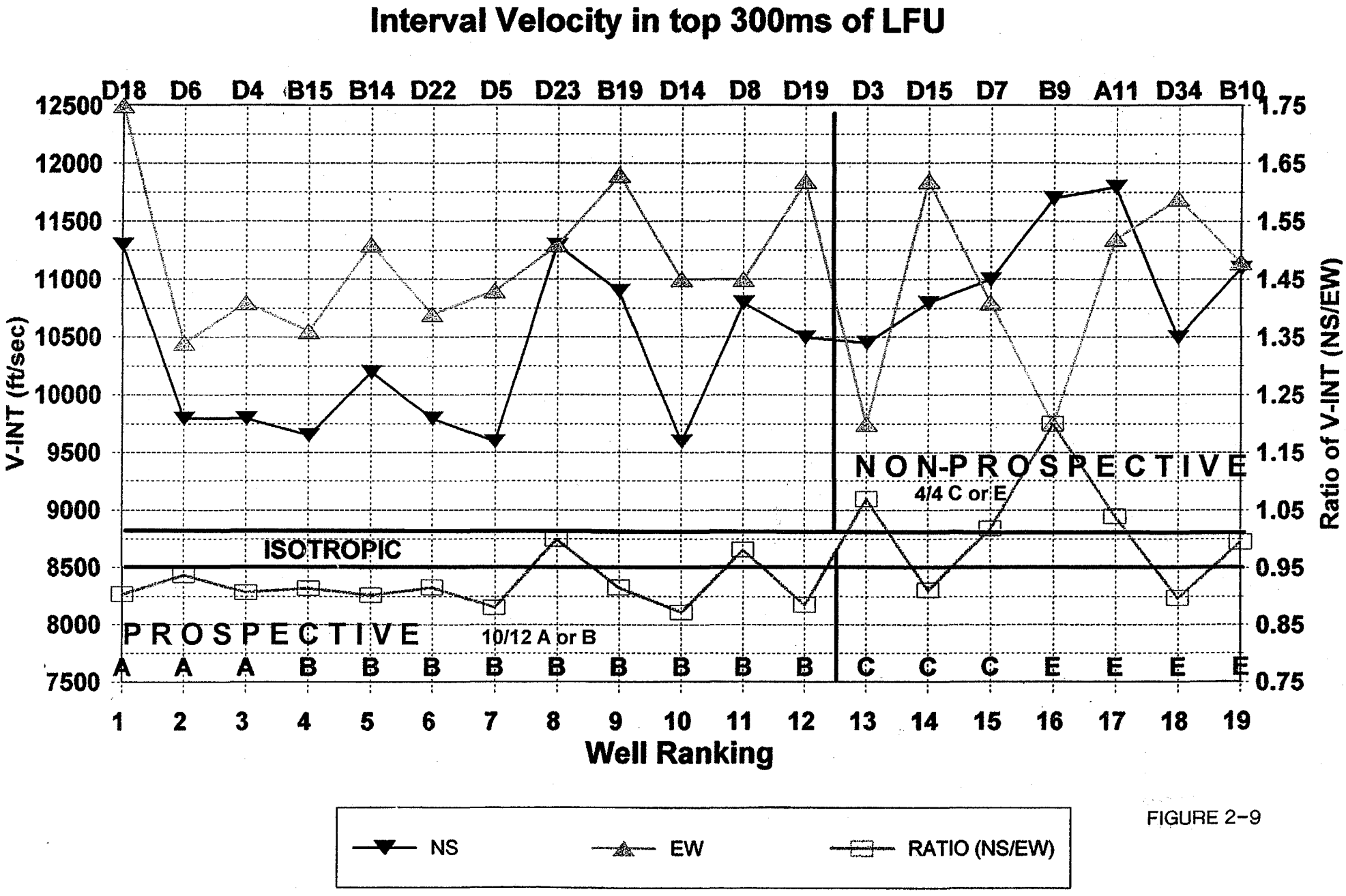
Interval Velocity in top 300ms of LFU
D18 D6 D4 B15 B14 D22 D5 D23 B19 D14 D8 D19 D3 D15 D7 B9 A11 D34 B10
12500
12000
11500
11000
10500
10000
9500
9000
8500
8000
7500
V-INT (ft/sec)
1.75
1.65
1.55
1.45
1.35
1.25
1.15
1.05
0.95
0.85
0.75
Ratio of V-INT (NS/EW)
NON-PROSPECTIVE
4/4 C or E
ISOTROPIC
PROSPECTIVE
10/12 A or B
A A A B B B B B B B B B C C C E E E E
1 2 3 4 5 6 7 8 9 10 11 12 13 14 15 16 17 18 19
Well Ranking
NS
EW
RATIO (NS/EW)

FIGURE 2-9

3.0 PARAXIAL RAY-TRACING MODELING

The paraxial ray-tracing code was acquired from MIT in late September. The code was tested against benchmark AVO results and minor modifications made to adapt it better to the present modeling tasks. These tests are presently being extended toward cases that more closely resemble the Wind River Basin field, for example, the AVO response of an anisotropic syncline. Concurrently, a detailed reproduction of the 37 square mile 3-D experiment is being constructed from the shot-receiver configurations recorded in the observer's logs and the horizon picks from the seismic interpreters. When completed, the paraxial ray-tracing code will be able to simulate the AVO response of the top of the Lower Fort Union formation for a variety of structural models, including both large- and small-scale structures (e.g., folds and fracture families, respectively). These simulations will be compared to the observed AVO to test the hypothesis that large-scale structures can influence conclusions reached about small-scale structure.

4.0 TECHNOLOGY TRANSFER

A summary of the technology transfer events in the third quarter of 1996 is given below.

Blackhawk was contacted by Mr. Abdul Fattah Al-Dajani of the Colorado School of Mines for the purpose of using the 37 square mile 3D data for his studies of azimuthal variation of velocity. Mr. Al-Dajani works in the same group as Dr. Ilya Tsvankin and Andreas Ruger, who have previously analyzed the amplitude characteristics of the 37 square mile 3-D dataset. Mr. Al-Dajani prepared an outline for the owner/operator of the work he intends to perform on the data, and the owner/operator gave their permission for Mr. Al-Dajani to use the 37 square mile 3-D dataset for his research.

An abstract was submitted and accepted for oral presentation at the 1997 SAGEEP conference, sponsored by the Environmental and Engineering Geophysical Society, to be held in April, 1997. The title of the abstract is "Mapping Bedrock Topography with Seismic Refraction at an Oil and Gas Field: A Comparison of Engineering and Petroleum Exploration Methods at a Site in the Wind River Basin of Wyoming."

An abstract for a poster paper was also submitted to the AAPG for their 1997 annual convention to be held in April, 1997. The title is "Detection of Naturally Fractured Tight Gas Reservoirs: Case Histories from the Uinta and Wind River Basins Using 2-D and 3-D Seismic Data."

Copies of two abstracts submitted during this quarter are attached.

4.1 Abstracts

Mapping Bedrock Topography with Seismic Refraction at an Oil and Gas Field: A Comparison of Engineering and Petroleum Exploration Methods at a Site in the Wind River Basin of Wyoming.

David Phillips and Bart Hoekstra, Blackhawk Geometrics

Bedrock topography is often the main factor controlling groundwater flow and pathways for contaminant migration. Over the last ten years, seismic 3-D surveys have been conducted at many producing oil and gas fields for definition of the hydrocarbon bearing units at thousands of feet in depth. A significant by-product of the 3-D survey is the refraction statics solution, which is used to remove near surface time delays during data processing.

The main goal of the refraction statics is to calculate time delays, rather than bedrock depth; and because of this, some assumptions are made which greatly impact the depth solution. One such assumption is that the velocity of the uppermost layer (V1) can be held constant. This causes serious deviations in bedrock depth and shape where V1 varies laterally.

Several shots were extracted from the 3-D dataset (lying along one receiver line in the 3-D receiver patch) to create a 2-D line. The first breaks from these shots were re-picked and analyzed using the Generalized Reciprocal Method (GRM). The largest source of error in this type of analysis is the first break picking of the near offset traces. These arrivals can be severely smeared by the large receiver arrays used in exploration surveys, and this smearing causes uncertainty in the calculation of V1.

At the same location of the extracted 2-D GRM line, a shallow refraction line was recorded using an engineering seismograph and 60 receivers spaced at 10 feet. The first breaks were picked, and depth profiles were calculated using the GRM.

A comparison of the three refraction profiles will be shown where discrepancies in depth and velocity can be analyzed. Displays of the seismic data will also given, showing variations in frequency and signal to noise ratio for the two data types.

Detection of Naturally Fractured Tight Gas Reservoirs: Case Histories from the Uinta and Wind River Basins Using 2-D and 3-D Seismic Data

PHILLIPS, DAVE, Blackhawk Geometrics, Golden, CO; HELOISE B. LYNN and MICHELE SIMON, Lynn, Inc., Houston, TX; and RICHARD VAN DOK, Western Geophysical, Denver, CO

The goal of the two U.S. DOE research projects directed by Blackhawk Geometrics, contract no. DE-AC21-92MC28135 and DE-AC21-94MC31224, is the detection of gas filled fractures using seismic methods. If highly fractured areas can be located using seismic techniques prior to drilling, it can greatly benefit field development. Shear wave seismic detects fractures, but it is expensive to acquire. If P-wave data can also detect fractures, the costs of finding fractured areas will be significantly reduced. In the Uinta Basin, two multicomponent seismic lines and a multicomponent VSP were used to define fractures in the Upper Green River Formation. The azimuthal difference of the P-wave AVO gradients showed open fracture directions consistent with the shear wave and VSP data. The dominant fracture direction at the Wind River Basin study area is East-West, and this information was used to design a processing sequence which splits the 3-D dataset into two subsets. Compressional waves which travel parallel to the dominant fracture direction will not sense the fractures, while compressional waves which travel perpendicular to the dominant fracture direction will sense the maximum influence of the fractures. The subsets were processed independently, and the azimuthally variant seismic attributes were compared to production information from wells to calibrate the seismic attributes to production.